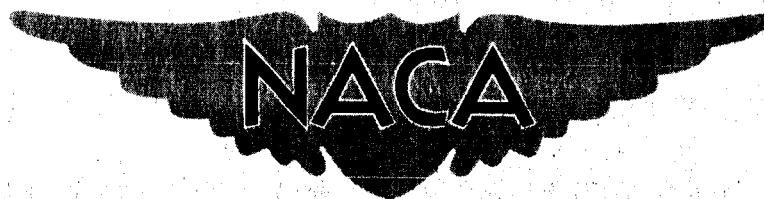


NACA RM SL54H02



# RESEARCH MEMORANDUM

for the

Bureau of Aeronautics, Department of the Navy

ZERO-LIFT DRAG OF THE CHANCE VOUGHT REGULUS II MISSILE AT  
MACH NUMBERS BETWEEN 0.8 AND 2.2 AS DETERMINED FROM THE  
FLIGHT TESTS OF TWO 0.12-SCALE MODELS

REPORT NO. NACA AD 398

By James D. Church

Langley Aeronautical Laboratory  
Langley Field, Va.

CLASSIFIED DOCUMENT

This material contains information affecting the National Defense of the United States within the meaning of the espionage laws, Title 18, U.S.C., Secs. 793 and 794, the transmission or revelation of which in any manner to an unauthorized person is prohibited by law.

## NATIONAL ADVISORY COMMITTEE FOR AERONAUTICS

WASHINGTON

DEC 27 1964

N65-86193

(ACCESSION NUMBER)

16  
(PAGES)

(THRU)

(CODE)

(NASA CR OR TMX OR AD NUMBER)

(CATEGORY)

DECLASSIFIED BY AUTHORITY OF NASA  
CLASSIFICATION CHANGE NOTICES NO. 1  
DATE 5-26-65 ITEM NO. 33

DECLASSIFIED BY AUTHORITY OF NASA  
CLASSIFICATION CHANGE NOTICES NO. 1  
DATE 5-26-65 ITEM NO. 33

DECLASSIFIED

## NATIONAL ADVISORY COMMITTEE FOR AERONAUTICS

## RESEARCH MEMORANDUM

for the

Bureau of Aeronautics, Department of the Navy

ZERO-LIFT DRAG OF THE CHANCE VUGHT REGULUS II MISSILE AT  
MACH NUMBERS BETWEEN 0.8 AND 2.2 AS DETERMINED FROM THE  
FLIGHT TESTS OF TWO 0.12-SCALE MODELS

TED NO. NACA AD 398


By James D. Church

## SUMMARY

Two noninstrumented 0.12-scale models (with internal flow) of the Chance Vought Regulus II missile were flight tested to investigate drag characteristics of the missile for a range of Mach numbers from 0.8 to 2.2. Measured total-drag-coefficient data were reduced to external-drag-coefficient data by using qualitative estimates of internal and base-drag coefficients. Both the total drag as measured on the two models, the external drag of the present tests, and some unpublished preliminary wind-tunnel test data show that differences in the drag level occurred for a range of supersonic Mach numbers between 1.3 and 2.0. These differences in the drag, believed to be caused by the additive drag characteristics of the inlet, leave the exact drag level of the configuration investigated in question.

## INTRODUCTION

At the request of the Bureau of Aeronautics, Department of the Navy, the National Advisory Committee for Aeronautics has made an investigation of the drag characteristics near zero lift of the Chance Vought Regulus II missile (XRSSM-N-9). This drag investigation utilized two 0.12-scale rocket-boosted models, which were flown in the speed range proposed for the full-scale missile. These flight tests were conducted at the Langley Pilotless Aircraft Research Station at Wallops Island, Va.



This paper presents the results obtained from the flight tests of two noninstrumented drag models having internal flow. Measured total-drag coefficients are presented for a range of Mach number from 0.8 to 2.2. In addition, the variation of external-drag coefficients has been estimated over the same speed range by use of qualitative values of base and internal drag.

#### SYMBOLS

x	longitudinal distance, measured from the nose, in.
L	model length, 81.50 in.
MGC	wing mean geometric chord, 0.873 ft
A	cross-sectional area, sq in.
S	total wing area (including body intercept), 2.08 sq ft
M	Mach number
q	dynamic pressure, lb/sq ft
R	Reynolds number (based on MGC)
$m/m_0$	ratio of mass flow of air through the duct to mass flow of air through a free-stream tube of area equal to projected inlet frontal area (6.68 sq in.)
$C_D$	drag coefficient, Drag/qS

#### Subscripts:

t	total
i	internal
b	base pressure
e	external

## MODELS AND TESTS


Two models of the Regulus II missile were tested. Each model was a 0.12-scale version of the full-scale missile with the exception that it had a smaller duct exit and, hence, a larger base annulus (7.06 sq in.) in order to more nearly simulate the internal flow of the missile. A three-view sketch of the 0.12-scale model is presented in figure 1. The fuselage consisted of a nose section (contour coordinates presented in table I) with a  $2^\circ$  body "flat" that led into an underslung boundary-layer bleed and inlet system.

The inlet face was included in a plane swept forward  $43.8^\circ$  and the initial internal lip angle was  $14.3^\circ$  (design  $M = 2.03$ ). Flow from the inlet went through a double minimum duct which exhausted at the base of the fuselage. The cross-sectional area of the duct was reduced from the lip to a minimum, increased to a constant area, then reduced again to a second and smaller minimum near the exit of the duct (see table II). The boundary-layer bleed was split at the intake to discharge from ports located under each wing. The wing and tail surfaces were mounted on the afterbody and had slightly modified biconvex airfoil sections, as well as blunt trailing edges (see table I).

The nose section, the casting for the inlet-boundary-layer bleed, and the solid wing and tail surfaces were of aluminum alloy. The duct in the wooden afterbody was fabricated from fiberglass reinforced with a short aluminum sleeve inserted in the exit. A plot of the longitudinal distribution of cross-sectional area is presented in figure 2. The area distribution of this figure has been adjusted for mass flow ratio by subtracting the equivalent free-stream-tube area at  $M = 1.0$  (projected inlet frontal area multiplied by  $m/m_0$ ) as suggested in reference 1.

The two models, which were identical within construction tolerances, were accelerated to peak Mach number by two different booster-rocket systems. Model 1 was propelled by a single ABL Deacon booster and model 2 by a double Deacon booster. Photographs of the model and the two model-booster combinations are shown in figure 3.

The models were flown near zero lift by virtue of a center of gravity that was far forward. The total drag was computed from data obtained during the decelerating portion of flight that followed separation from the booster. This drag computational method (presented in ref. 2) utilized the following measurements of each flight: model velocity by CW Doppler radar (corrected for flight-path curvature and winds aloft), model position in space by a radar tracking set, and atmospheric data by radiosonde.



The possible random error of the data is estimated from previous experience to be within the following limits:

	<u>Subsonic</u>	<u>Supersonic</u>
M . . . . .	$\pm 0.010$	$\pm 0.005$
$C_{Dt}$ . . . . .	$\pm 0.003$	$\pm 0.002$

Although these estimates apply to the absolute value of the quantities, the probable error in these variables can be considered to be roughly one-half as large as that shown.

The variation of Reynolds number with Mach number for both model flights is presented in figure 4. Since an estimate of internal drag will be presented, the estimated mass-flow ratio  $m/m_0$  is also shown on this figure.

## RESULTS AND DISCUSSION

The measured total-drag coefficients for the two models tested are presented in figure 5; also shown are qualitative estimates of base and internal drag coefficients and the corresponding external drag coefficients.

### Total Drag

The total-drag-coefficient ( $C_{Dt}$ ) curves shown in figure 5(a) indicate that the 0.12-scale model had a drag-rise Mach number of approximately 0.95. The total drag coefficients of models 1 and 2 were in good agreement between  $M = 1.16$  and  $M = 1.37$ ; and it is interesting to note that  $C_{Dt}$  approached the same level for each model at its highest test Mach number. However, in the Mach number range between 1.4 and 2.0, the drag levels of the two models differ by an amount larger than the estimated accuracy of the data. It is believed that this discrepancy in  $C_{Dt}$  may have resulted from differences in the mass-flow rates of the two models.

### External Drag

In an attempt to extend the usefulness of the test results, these total-drag values were reduced to external drag by subtracting qualitative estimates of the internal and base drag of each model. The



estimated mass-flow ratio  $m/m_0$  of the models used in the present tests is presented in figure 4. Values of  $m/m_0$  and total pressure recovery were obtained over the intermediate Mach number range of the present tests from unpublished wind-tunnel results supplied by Chance Vought. These test points were then faired and extended over the required Mach number range by use of calculated values of flow parameters - these calculated values were obtained by assuming the duct recovery and the choking at the minimum section near the exit. Values of the internal drag coefficient, as usually defined for internal flow systems,  $C_{D_i}$ , were determined by substituting the estimated flow parameters into the equation contained in the appendix of reference 3. Further calculations indicated that for a fairly wide variation in flow rate the associated changes in the magnitude of  $C_{D_i}$  were quite small when compared to the magnitude of  $C_{D_t}$ . The single  $C_{D_i}$  curve presented in figure 5(b) is therefore considered to be a good qualitative estimate for both models.

Base pressure drag  $C_{D_b}$  was empirically estimated from a compilation of results obtained from rocket-propelled models. These results consisted of base pressure measurements made on numerous ducted models with base annuli that were flown with a choked exit condition. The annulus area of the 0.12-scale model was used in conjunction with these base-pressure coefficients to yield the qualitative estimate of  $C_{D_b}$  shown in figure 5(b) for both models.

The external drag  $C_{D_e}$ , also shown on figure 5(b), was obtained by subtracting the calculated  $C_{D_i}$  and  $C_{D_b}$  values from the  $C_{D_t}$  curves of both models. Also presented in figure 5(b) are preliminary test points obtained in the Langley 4- by 4-foot supersonic pressure tunnel on a ducted 0.065-scale model of the missile. These data are presented for the mass-flow ratios estimated for the flight models, shown in figure 4. The test Reynolds numbers based on the model mean geometric chord (5.78 in.) were  $R = 1.91, 1.83, \text{ and } 1.57 \times 10^6$  for  $M = 1.41, 1.61, \text{ and } 2.01$ , respectively.

As shown in figure 5, the difference in the estimated external-drag level of the two models is reflected into the measured total drag. Moreover, a comparison of the tunnel data and the rocket model data shows these unexpected differences in the external drag which indicate that the inlet may not be functioning properly. It is believed that at any particular Mach number the flow rates of each flight model differed from the assumed  $m/m_0$  values presented in figure 4. As previously stated, internal-drag variations resulting from differences in flow

rate are small compared with variations of the total drag; however, it is believed that changes in flow rate and duct characteristics could cause appreciable variation of the external drag as a result of the influence of scoop spillage. This additive drag due to scoop spillage is considered part of the external drag, and by virtue of such factors as inlet shock oscillations, changes in trim angles, small differences in geometry, etc., could achieve sufficient magnitude to account for the discrepancies encountered in the external drag.

#### SUMMARY OF RESULTS

The results of flight tests of two 0.12-scale models of the Chance Vought Regulus II missile are presented for a range of Mach numbers from 0.8 to 2.2. Measured total-drag-coefficient data were reduced to external-drag-coefficient data by using qualitative estimates of internal and base drag coefficient. The external drag of the present tests and some preliminary wind-tunnel test points showed a difference in the drag level for the range of supersonic Mach numbers between 1.3 and 2.0. These differences in the drag are believed to be caused by the additive drag characteristics of the inlet; determination of the exact drag level of this configuration will therefore require additional data.

Langley Aeronautical Laboratory,  
National Advisory Committee for Aeronautics,  
Langley Field, Va., July 15, 1954.

*David B. Stone*  
for James D. Church  
Aeronautical Research Scientist

Approved:

*Joseph A. Shortal*  
Joseph A. Shortal  
Chief of Pilotless Aircraft Research Division

JKS



## REFERENCES

1. Hall, James Rudyard: Comparison of Free-Flight Measurements of the Zero-Lift Drag Rise of Six Airplane Configurations and Their Equivalent Bodies of Revolution at Transonic Speeds. NACA RM L53J21a, 1954.
2. Wallskog, Harvey A., and Hart, Roger G.: Investigation of the Drag of Blunt-Nosed Bodies of Revolution in Free Flight at Mach Numbers From 0.6 to 2.3. NACA RM L53D14a, 1953.
3. Merlet, Charles F., and Putland, Leonard W.: Flight Determination of the Drag of Conical-Shock Nose Inlets with Various Cowling Shapes and Axial Positions of the Center Body at Mach Numbers From 0.8 to 2.0. NACA RM L54G21a, 1954.





TABLE I.- PERTINENT MODEL COORDINATES

Body nose contour (in.)	
Station	Radius
0	0
1.20	.365
2.76	.668
3.60	↑
4.80	Straight
6.00	line
7.20	↓
7.92	1.404
8.40	1.471
9.60	1.623
10.80	1.726
12.00	1.891
13.20	2.011
14.40	2.125
15.60	2.233
16.80	2.336
18.00	2.433
19.20	2.526
20.40	2.613
21.60	2.695
22.80	2.771
24.00	2.841
25.20	2.904
26.40	2.959
27.00	2.982
27.54	3.000

Wing airfoil contour (percent chord)	
X	Y
0	0
.10	.0057
.15	.0084
.20	.0109
.25	.0132
.30	.0152
.35	.0169
.40	.0183
.45	.0193
.50	.0199
.537	.0200
.60	.0196
.65	.0187
.70	.0174
.75	.0157
.80	.0135
.85	.0110
.90	.0083
.95	.0052
1.00	.0020
Straight-line fairing from tangent to con- stant leading-edge radius of 0.004 inch to tangent of 0.10 chord.	

TABLE II.- DUCT AREA PERPENDICULAR TO DUCT CENTER LINE

Station (in.)	Area (sq in.)
36.54	6.68
39.42	5.37
40.45	5.30
44.33	5.82
46.35	6.27
48.63	6.73
51.20	6.95
54.07	7.02
74.45	7.02
75.21	6.38
75.63	5.57
76.01	5.15
81.50	5.24
Area at first station is the projected inlet frontal area.	

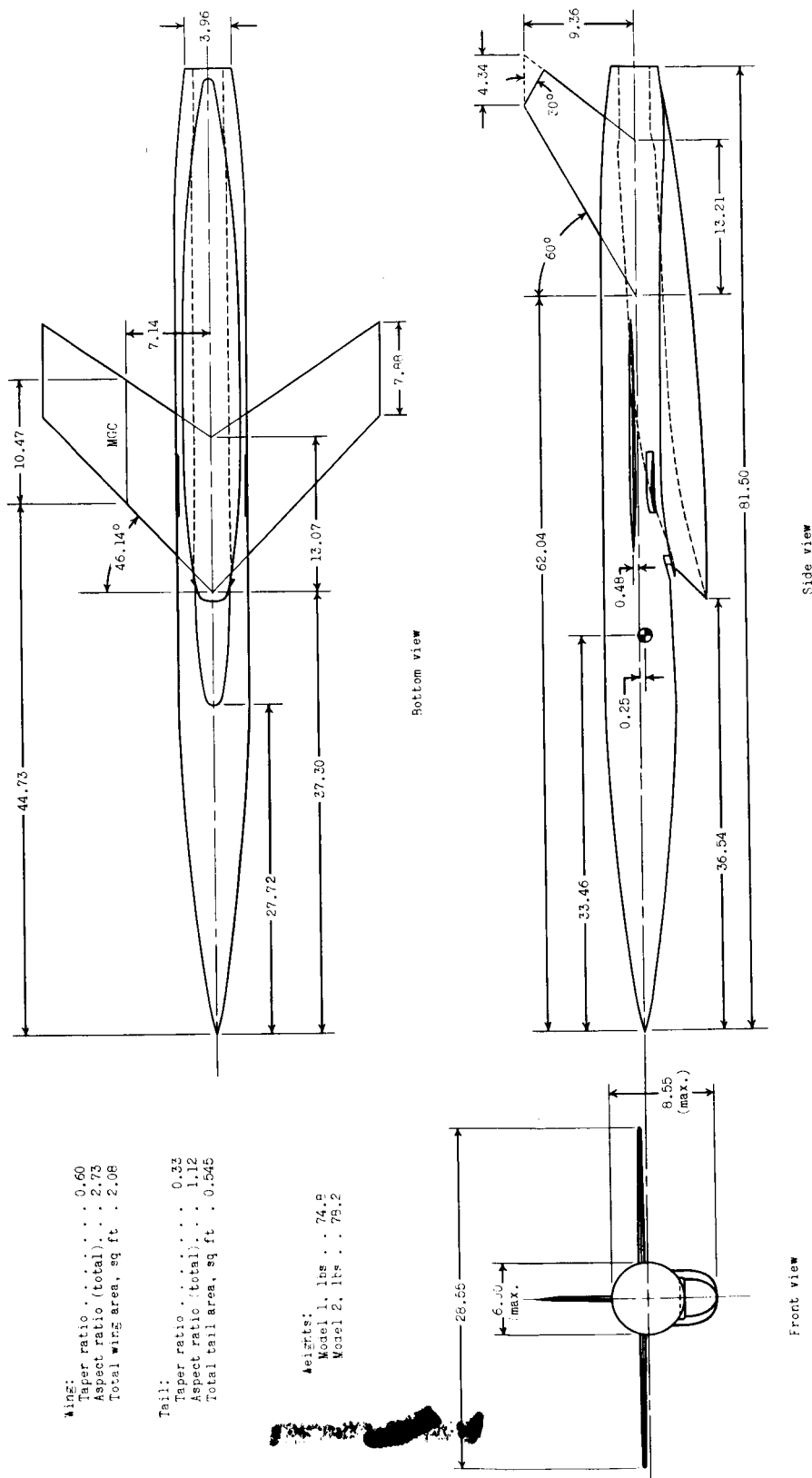


Figure 1.- General arrangement of 0.12-scale model. (All dimensions are in inches.)

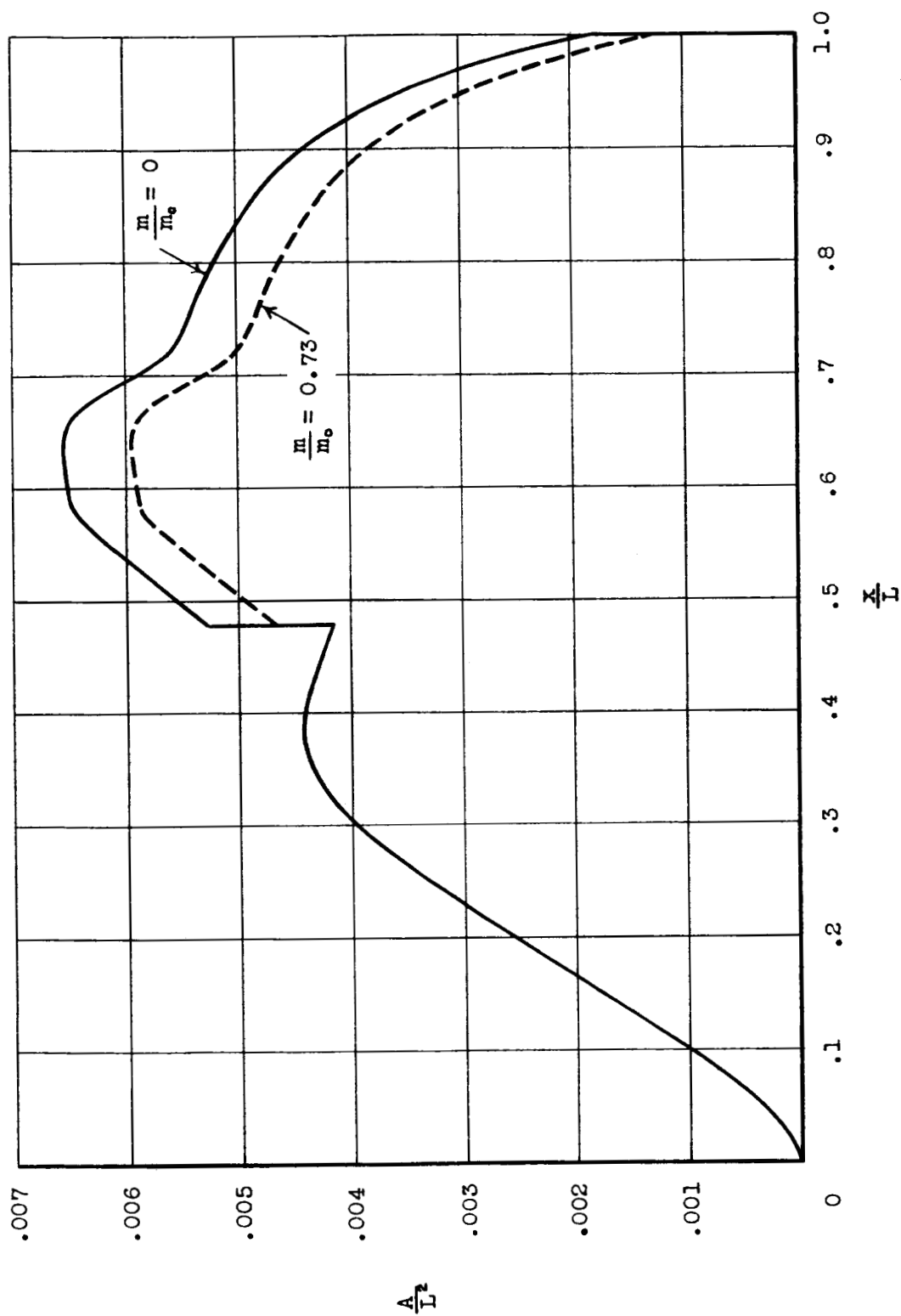
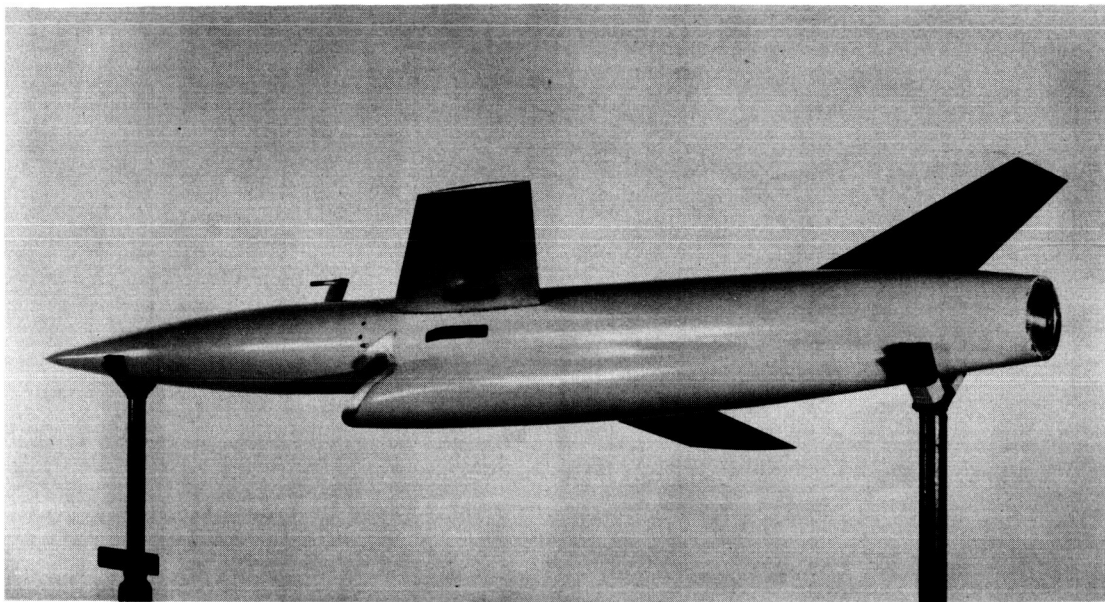
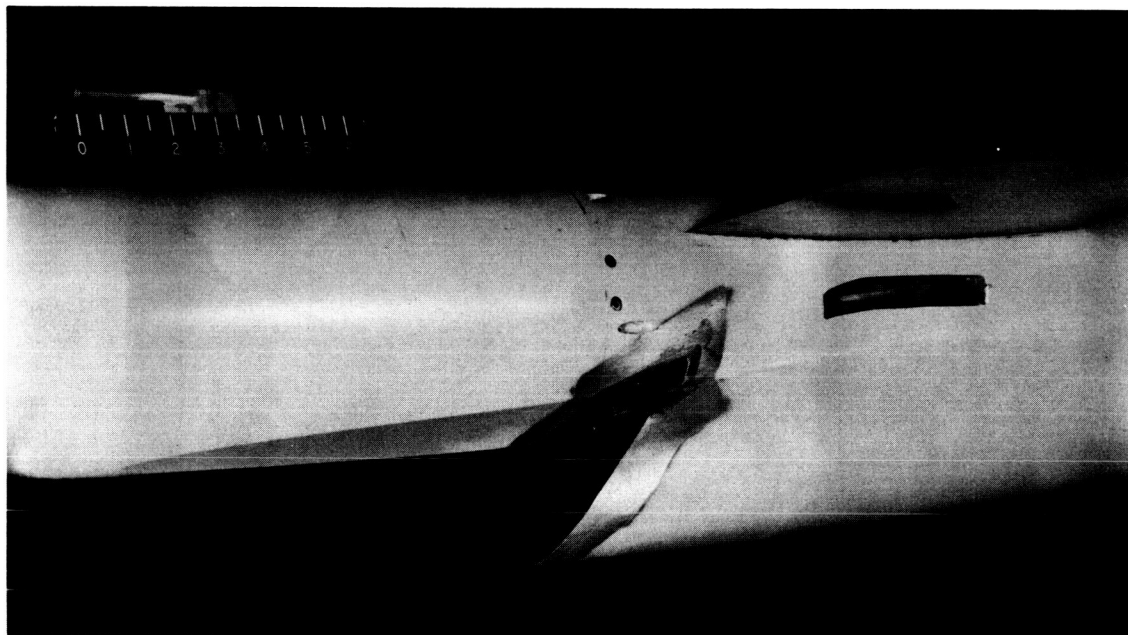


Figure 2.- Longitudinal distribution of cross-sectional area.



(a) Three-quarter-rear view.

L-84522

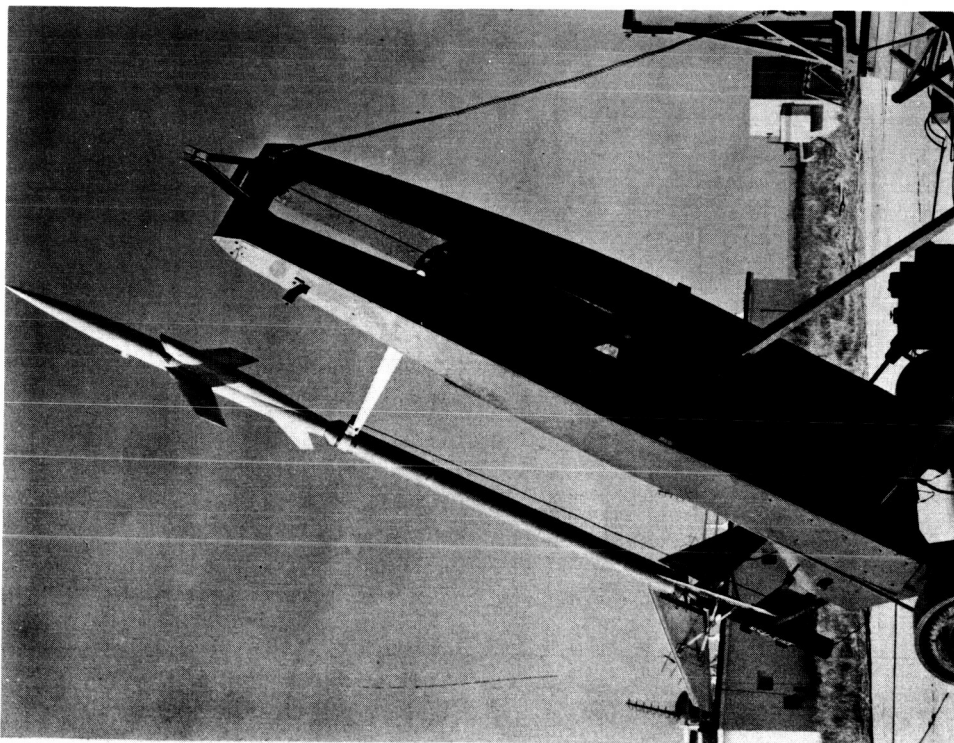


L-84521

(b) View of inlet and boundary-layer bleed arrangement.

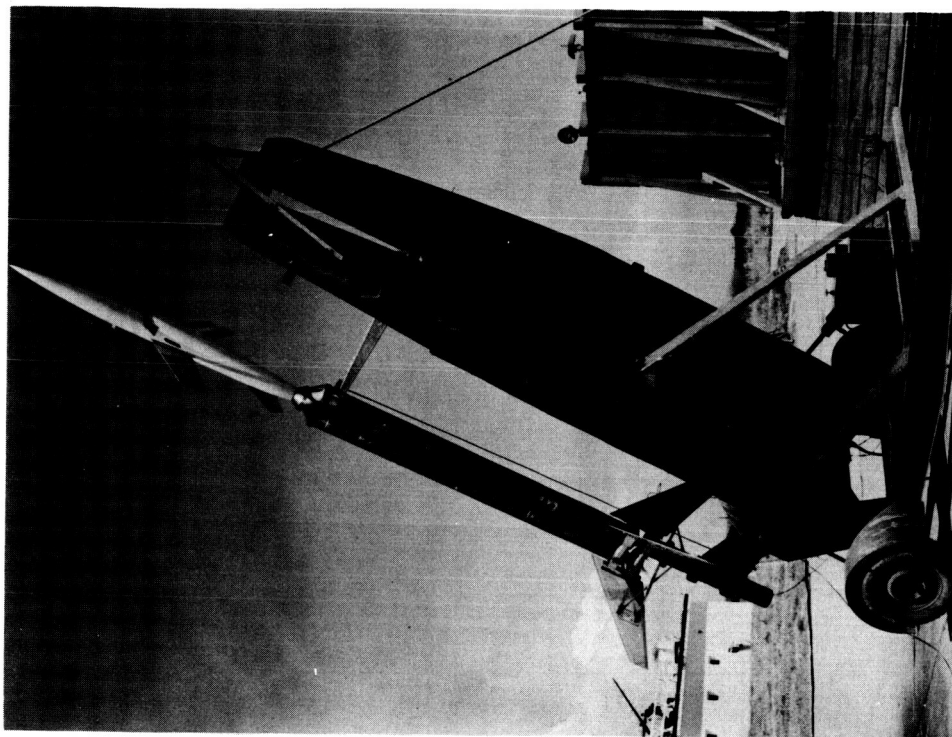
Figure 3.- Photographs of the models.





L-84167

(c) Model 1 prior to launching.



L-84630

(d) Model 2 prior to launching.

Figure 3.- Concluded.

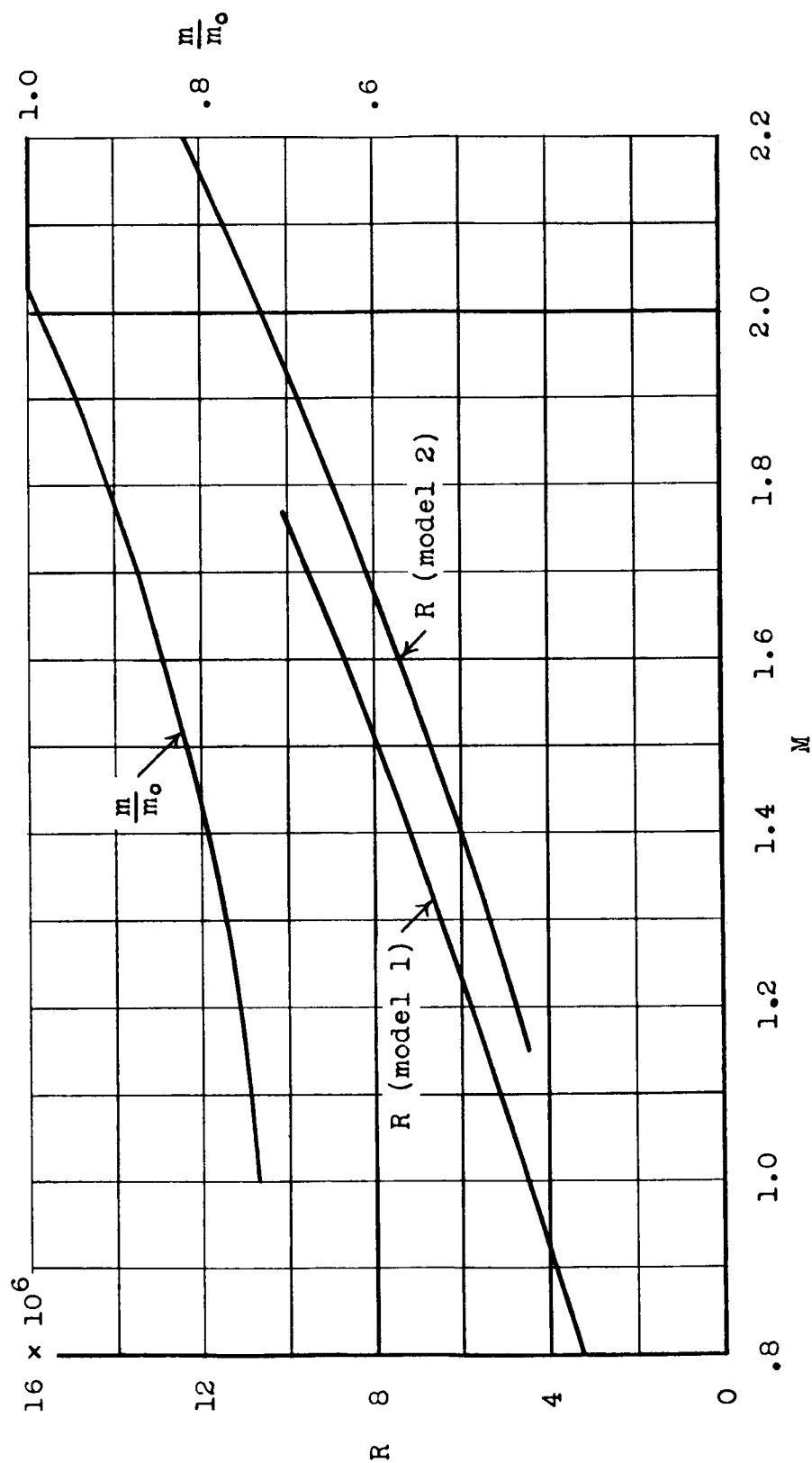
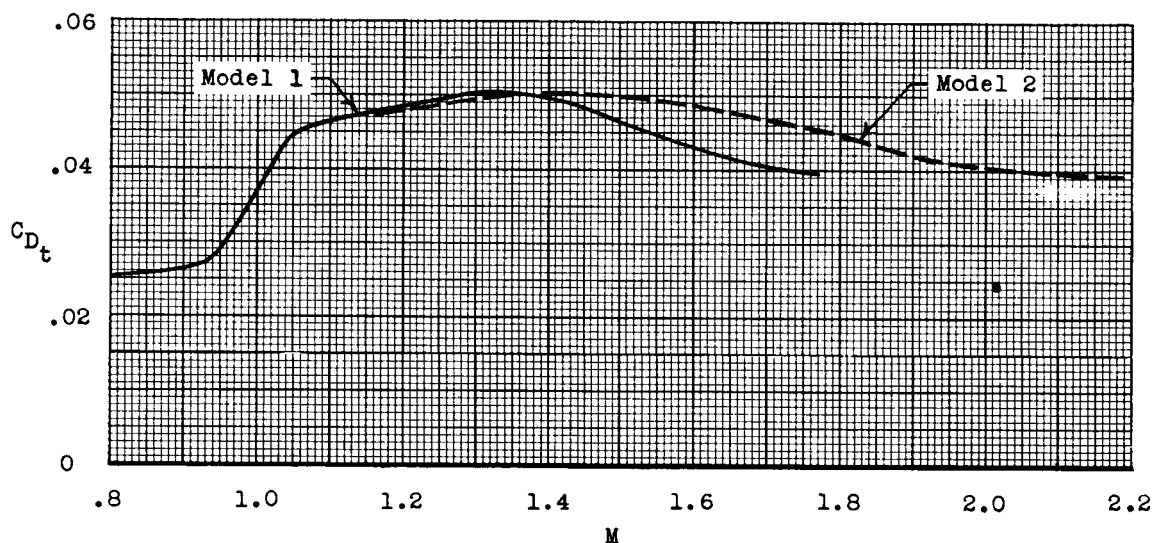
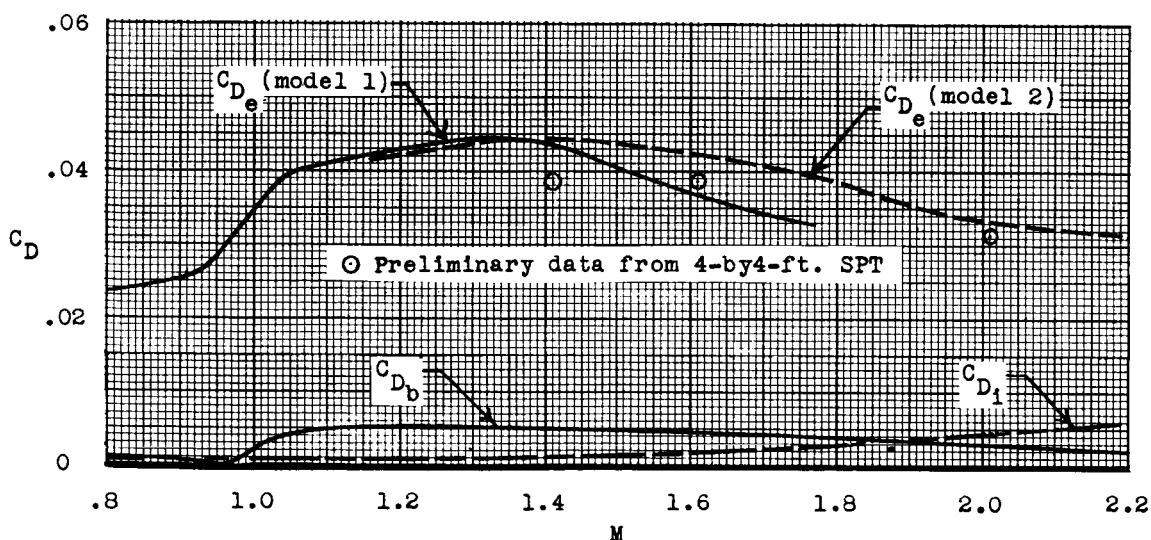


Figure 4.- Variation of Reynolds number and estimated mass-flow ratio with Mach number.



(a) Measured total-drag coefficient.



(b) Estimated external-drag coefficient and estimated internal and base-pressure drag coefficients.

Figure 5.- Variation of measured and estimated drag coefficients with Mach number.